Polymer 53 (2012) 4019–4024

Contents lists available at SciVerse ScienceDirect

Polymer

journal homepage: www.elsevier.com/locate/polymer

Synthesis and characterization of nanocomposites of thermoplastic polyurethane with both graphene and graphene nanoribbon fillers

Sergio Scognamillo [a], Emilia Gioffredi [b], Massimo Piccinini [c], Massimo Lazzari [d], Valeria Alzari [a], Daniele Nuvoli [a], Roberta Sanna [a], Daniele Piga [a], Giulio Malucelli [b,**], Alberto Mariani [a,*]

[a] Dipartimento di Chimica e Farmacia, Università di Sassari, and Local INSTM Unit, Via Vienna 2, 07100 Sassari, Italy
[b] Dipartimento di Scienza Applicata e Tecnologia, Politecnico di Torino, sede di Alessandria, and Local INSTM Unit, Via T. Michel 5,15121 Alessandria, Italy
[c] Porto Conte Ricerche S.r.l., SP 55 km 8.400 Loc. Tramariglio, 07041 Alghero (SS), Italy
[d] Centre for Research in Biological Chemistry and Molecular Materials (CIQUS) c. Jenaro de la Fuente s/n, Campus Vida, University of Santiago de Compostela, 15782 Santiago de Compostela, Spain

ARTICLE INFO

Article history:
Received 26 March 2012
Received in revised form
20 June 2012
Accepted 8 July 2012
Available online 24 July 2012

Keywords:
Graphene
Nanocomposites
Thermoplastic polyurethanes

ABSTRACT

Thermoplastic polyurethane (TPU) nanocomposites containing graphene and graphene nanoribbons were obtained by polymerizing 1,4-butanediol with two diisocyanates (namely, 1,6-hexane diisocyanate or isophorone diisocyanate), in which the nanofillers were previously dispersed. Raman spectroscopy and Transmission Electron Microscopy demonstrated the formation of few-layer graphene and graphene nanoribbons dispersed in the monomers. At variance to the methods commonly reported in literature, that used in this work consists of the direct exfoliation of graphite without any chemical manipulation. Apart from the obvious cost and ease advantages, the so-obtained graphene does not contain any carboxy or alkoxy groups formed during the exfoliation process, which, at variance, are typically present in the most commonly reported methods. This finding paves the way toward the large-scale production of graphene and its nanoribbons, which are considered even more interesting than graphene itself for many potential applications. The obtained nanocomposites show a peculiar thermal and rheological behavior due to the presence of the nanofillers and to their reinforcing or plasticizing effect exerted on the TPU matrices.

1. Introduction

Graphene, one of the most exciting nanomaterials discovered in the last years, is becoming the key-stone of a plethora of new nanomaterials, thanks to its unique physical properties [1–4]. Several approaches have been explored for producing dispersions of mono-layer graphene [5]. Most of them are based on the oxidation of graphite to graphite oxide, its dispersion to get graphene oxide and the reduction of this latter [6–8]. However, only the epoxide groups are involved in this latter process, unlike COOH and OH groups, which are linked to the graphene edges. As a matter of the fact, the so-obtained "graphene" is one that contains a certain number of oxidized carbons, and consequently is characterized by properties that are different from those that real graphene may exhibit [9].

Coleman et al. opened a new route obtaining graphene sheets by direct graphite exfoliation in *N*-methylpyrrolidone (NMP) and achieving a graphene concentration equal to 0.01 mg mL^{-1} [10–16].

Pursuing this strategy, we were able to achieve the highest graphene concentration reported so far by dispersing graphite in a suitable ionic liquid [17], and lately in a significant number of liquid media that were polymerized, thus obtaining the corresponding polymer nanocomposites in a much easier and efficient way than those previously reported in the literature [18,19]. More specifically, we prepared the first graphene-based polymer composite by direct polymerization of the liquid monomer, in which this nanofiller was obtained by graphite sonication, thus avoiding any graphene recovery in the solid state and, consequently, any possible reaggregation phenomena [19,20].

Due to their versatile properties, thermoplastic polyurethanes (TPUs) have been widely used in industrial applications such as coatings, paintings and foams [20–22]; furthermore, some TPUs show biodegradability, which makes them suitable as biomaterials [20,23]. The tuning of TPU properties as hydrophilicity, glass transition temperature, hydrolytic stability and biological compatibility

* Corresponding author. Tel.: +39 (0)792 29556; fax: +39 (0)79229559.
** Corresponding author. Tel.: +39 (0)131 229369; fax: +39 (0)131 229399.
E-mail addresses: giulio.malucelli@polito.it (G. Malucelli), mariani@uniss.it (A. Mariani).

0032-3861/$ – see front matter © 2012 Elsevier Ltd. All rights reserved.
http://dx.doi.org/10.1016/j.polymer.2012.07.020

can be achieved by changing the structure and sequence of hard and soft segments present in the polymer [24–27].

Taking into consideration both the polymer versatility and the peculiar properties of graphene, in the present paper we report for the first time the preparation of graphene/TPU nanocomposites through the polymerization of suitable diisocyanate and diol pairs, in which graphene was dispersed according to our previously published method [17–19]. To this aim, two diisocyanates (namely, 1,6-hexane diisocyanate (HDI) and isophorone diisocyanate (IPDI)) were allowed to react with 1,4-butanediol (BD).

A large amount of graphene nanoribbons, thin strips of graphene just a few atoms wide, were also obtained. For their peculiar features, they are considered even more interesting than graphene itself in many advanced applications. In particular, at variance to graphene, which is known to be a zero-gap semiconductor with finite minimum conductivity, a feature that limits its use in conventional digital logic applications, a bandgap opens up in narrow graphene nanoribbons through spatial confinement and edge effects [28]. Indeed, graphene nanoribbons exhibit interesting electronic and spintronic characteristics [29–33], especially quantum-confined bandgaps and magnetic edge states.

Graphene and/or its nanoribbons were successfully embedded in the obtained polymer matrix at various concentrations. The thermal and rheological behavior of the resulting nanocomposites were deeply investigated and correlated to the graphene content.

2. Experimental

2.1. Materials

BD (98%, $d = 1.047$ g mL^{-1}), HDI (98%, $d = 1.047$ g mL^{-1}), IPDI (98%, $d = 1.049$ g mL^{-1}), NMP, 1,2-dihydroxybenzene, Pyrocatechol (PC), dibutyltindiacetate (DBTDAc) and graphite flakes were purchased from Sigma Aldrich and used as received without further purification.

2.2. Graphene dispersions

A mixture of diisocyanates or diol (100 mL) and graphite flakes (5.0 wt.%, 5.00 g) was put into four different tubular plastic reactors (i.d.: 15 mm) and placed in an ultrasonic bath (Emmegi, 0.55 kW) for 24 h, at 40 °C. Then, the reactors were centrifuged for 30 min at 4000 rpm; the gray liquid phase containing graphene was then recovered.

2.3. Synthesis of the polyurethane nanocomposites

The dispersions of graphene were mixed together according to the following molar ratios: diisocyanate/diol (1:1), diisocyanate/DBTDAc (1:0.01), DBTDAc/PC (1:30) and diisocyanate/NMP (1:0.1). The mixtures were heated at 70 °C for 1 h, then cooled down to room temperature; finally, the solvent was removed by Soxhlet extraction and the obtained products analyzed.

2.4. Characterization techniques

Raman analyses were performed on graphene flakes obtained after vacuum filtration of the dispersions on polyvinylidene fluoride filters (pore size: 0.22 μm), with a BrukerSenterra Raman microscope, using an excitation wavelength of 532 nm at 5 mW. The spectra were acquired by averaging 5 acquisitions of 5 s with a 50× objective.

Transmission electron microscope (TEM) studies were performed on a JEOL JEM-1011 or a Libra 200 FE OMEGA, working with an accelerating voltage of 100 or 200 kV, respectively. Samples were prepared by dropping 20 μL of dispersion onto carbon-coated 400 mesh copper grids (15–25 nm carbon layer thickness, Ted Pella Inc.), and analyzed after solvent evaporation under vacuum at room temperature for 1 h. TEM images were also analyzed to evaluate the percentage of nanoribbons, i.e. graphene (planar) structures with a large aspect ratio, which may also be partially rolled up, in a series of at least 10 images per sample. Even though the total area covered by such number of images is very small to carry high statistical significance, it was sufficient to enlighten the presence of approximately a half of the few layers of graphene sheets with a large aspect ratio into the HDI/graphene dispersions. Ultrathin sections (nominal thickness of 80 nm) of polyurethane systems were cut at −80 °C using a Leica Ultracut UCT microtome with an EM-FCS cryo kit equipped with a diamond knife, and collected onto formvar-coated copper grids.

A Fourier transform infrared spectroscope (JASCO FT 480 spectrometer) was used for recording the FT-IR spectra of the samples. The powders were ground into a dry KBr disk and 32 scans at a resolution of 4 cm^{-1} were used to record the spectra.

Differential Scanning Calorimetry (DSC) measurements on the TPUs and their nanocomposites were performed by means of a Q100 Waters TA Instruments calorimeter, equipped with a TA Universal Analysis 2000 software. Two heating ramps, from 80 to 250 °C, with a heating rate of 10 °C min^{-1}, were carried out on dry samples: the first scan was performed to remove eventual residual solvent and to assess the extent of monomer conversion, which was always found complete (no exothermic peaks were found in the DSC traces).

Suitable disk specimens of the TPUs and their nanocomposites used for the rheological tests were obtained by compression molding at 100 bar and 160 °C. The rheological measurements were carried out on a strain-controlled rheometer (ARES, TA Instruments Inc., Waters LLC) with a torque transducer range of 0.2–2000 gf cm, using a 25 mm parallel plate geometry. The rheometer was equipped with a convection oven in nitrogen to avoid the thermal degradation of the samples. The rheological characterization was performed in frequency sweep tests at 160 °C (frequency ranging from 0.1 to 100 rad s^{-1}). Strain has been chosen in order to have a torque within the sensitivity of the instrument in the linear viscoelastic region. Furthermore, regression lines were used for interpolating viscosity data and giving an indication of the non-Newtonian behavior of the materials.

Several dilutions from the second aliquot of the above dispersions were analyzed by Ultraviolet (UV) spectrometry with a Hitachi U-2010 Instrument (1 cm cuvette). The above gravimetric data allowed us to determine the absorption coefficient: from a known volume of initial dispersion, several dilutions were carried out and the absorbance at a wavelength of 660 nm was measured [10,17,29]. Absorbance vs. concentration plots gave the absorption coefficient α.

3. Results and discussion

The first goal of the work was to obtain graphene by direct graphite sonication in the selfsame monomer to eventually polymerize: this was achieved without any physical or chemical manipulation and confirmed by experimental evidences. The first indication of the presence of graphene was provided by the occurrence of the Tyndall effect [33] in all the obtained monomer dispersions, which is a typical light scattering phenomenon confirming the presence of nanometric structures (Fig. 1).

The effect of the type of the monomer medium on the dispersion of graphene was investigated by adding a constant amount of graphite (5 wt.%) to BD or diisocyanates (HDI or IPDI) and obtaining the graphene concentrations reported in Table 1.

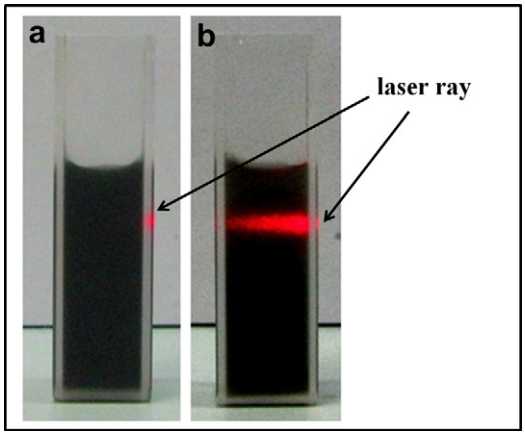

Fig. 1. Tyndall effect on dispersions of a) graphite and b) graphene in HDI.

In order to find the absorption coefficient α and the graphene concentration in such monomers, gravimetric analysis and UV spectroscopy measurements were carried out. The obtained data are collected in Table 2 and show a Lambert–Beer behavior for all the dispersions investigated. It is noteworthy that a concentration as high as 3.78 mg mL^{-1} was achieved when IPDI was used as the dispersing medium. However, also HDI and BD turned out to be very effective dispersing media (indeed, concentrations of 1.92 and 1.05 mg mL^{-1} were obtained in these monomers, respectively). It should be highlighted that these values are among the highest reported so far, independently on the solvent and method used for graphene preparation [10,12–14,19,34].

The formation of few-layer graphene sheets within the monomer dispersions was demonstrated by means of Raman spectroscopy. This technique is able to discriminate between graphite and graphene and allows determining the number of graphene layers within an acceptable error range. As shown in Fig. 2, the Raman signals for the dispersions obtained from HDI and IPDI are very similar to those of BD diol: all the spectra show the three typical graphene peaks at ~1334 cm^{-1} (D peak), ~1561 cm^{-1} (G peak) and ~2700 cm^{-1} (2D peak). In comparison with graphite, for which the diagnostic 2D peak consists of two components and the main peak is upshifted to 2714 cm^{-1}, the corresponding 2D peak of the monomers dispersions exhibit a sharp size and a downshifting, as it is expected in the presence of a few graphene layers. As far as the diisocyanates dispersions are concerned, the 2D signal is located at ca. 2680 cm^{-1}, whereas for BD it is around 2690 cm^{-1} (Fig. 2). In addition, the 2D peak downshifting is much more evident in the presence of diisocyanates: such behavior indicates that diisocyanates are capable to better disperse graphene with respect to diols. Besides, as expected, the D/G ratio values of graphene are higher than that of pristine graphite. Furthermore, it is worth mentioning that HDI and IPDI graphene dispersions are characterized by almost the same D/G ratio (ca. 0.2), while it is significantly higher in the BD system, thus indicating that a larger degree of disorder results from the dispersion of graphene in this latter liquid medium.

Table 1
Compositions, regression lines slope and flow behavior of the investigated TPUs.

Sample	Graphene [mg/mL]	Slope	Non-Newtonian behavior of the polymer system
HDI + BD systems			
A1	0	−0.98	Plastic
A2	0.80	−0.96	Plastic
A3	0.40	−0.98	Plastic
A4	0.20	−0.98	Plastic
A5	0.08	−0.99	Plastic
IPDI + BD systems			
B1	0	−0.53	Plastic
B2	1.14	−0.06	Newtonian
B3	0.28	−0.16	Newtonian
B4	0.11	−0.43	Pseudoplastic

Table 2
Graphene concentrations in the monomer dispersions and the corresponding UV absorption coefficients and Raman peaks (D, G, and 2D).

Monomer	Absorption coefficient, α [mL/mg m]	Graphene concentration [mg/mL]	D peak [cm^{-1}]	G peak [cm^{-1}]	2D peak [cm^{-1}]	D/G peak
BD	4164.7	1.05	1344	1572	2697	0.34
HDI	3211.2	1.92	1334	1561	2675	0.20
IPDI	8725.0	3.78	1344	1572	2686	0.19
Graphite	–	–	1347	1576	2314	0.11

The morphology of graphene sheets was assessed by TEM. All the dispersions showed the presence of large amounts of graphene sheets, such as those visible in Fig. 3a. Furthermore, in the case of IPDI, and in particular for the HDI/graphene dispersion, the formation of graphene nanoribbons was extensively observed (Fig. 3b). Differently from what reported in literature, in which very complicated methods for their obtainment are described [35–39], the formation of small amounts of graphene nanoribbons as a result of a simple graphite sonication in a polar liquid has been already reported by us [17] and lately by Ling et al. who also used a polymer surfactant [27]. In the present work, HDI turned out to be a very effective medium, as approximately half of the sheets resulted to be nanoribbons.

The graphene diisocyanate (HDI or IPDI) dispersions obtained by sonication were allowed to react with BD in order to get the two polyurethane systems. The adopted synthetic batch allowed achieving an almost full conversion of the monomers, as clearly indicated by Fourier transform infrared (FT-IR) spectroscopy (Fig. 4): indeed, the FT-IR spectra indicate the disappearance of the NCO signal (~2270 cm^{-1}) and the formation of the urethane groups (peaks at 3320 and 1720 cm^{-1}). In both cases, the graphene morphologies did not change after polymerization, as shown in Fig. 3c for the HDI-BD system. The completeness of the monomers conversion was also assessed through DSC analyses.

DSC analyses were performed in order to further confirm the completeness of the polymerization reaction and to assess the

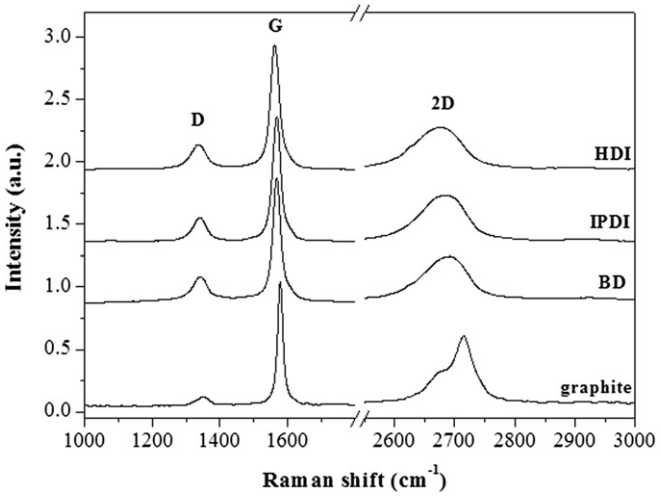

Fig. 2. Raman spectra of the graphene dispersions in the monomers: the diagnostic 2D peak (~2700 cm^{-1}), which, at variance to what happens for graphite, is symmetrical in graphene, indicates the presence of few-layer graphene.

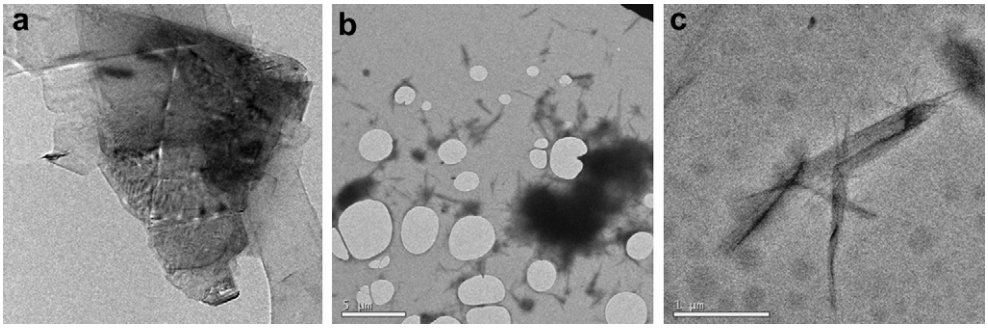

Fig. 3. TEM images of graphene structures in different dispersions: (a) few layers of graphene in an IPDI/graphene dispersion (diluted 1:100), (b) graphene nanoribbons in an HDI/graphene dispersion (diluted 1:10), and (c) HDI/BD polymer matrix containing graphene (0.80 mg/mL, sample A2).

ability of graphene to modify the thermal properties of the TPUs. As indicated in the experimental, all the DSC traces did not evidence any exothermic peak during the first heating up, thus further confirming the completeness of the polymerization reaction.

Fig. 5 plots the glass transition temperature (T_g) values for the HDI-BD and IPDI-BD polyurethane systems as a function of graphene concentration. It can be observed that the T_g of the IPDI-BD systems tends to increase even in the presence of very low amounts of graphene, reaching a sort of horizontal plateau as graphene concentration increases. This behavior indicates that, for this composite system, the nanofiller has the capability to interact with the matrix, acting as a reinforcing agent. The limit of the reinforcing capability can be probably ascribed to the lubrication effect exerted by graphene nanosheets, as already reported in the literature [18], which balances the reinforcing effect, so that T_g remains practically unchanged. On the other hand, for the HDI-BD systems, the lubrication/plasticization effect of the nanofiller overcomes its reinforcing feature, so that T_g decreases in the presence of very low amounts of graphene achieving a horizontal plateau (Fig. 5).

In Fig. 6, the storage (G′) and loss (G″) moduli are plotted as a function of frequency for the HDI-BD system. In addition, G′ is also included for some compositions containing graphene. The unfilled polymer (sample HDI-BD, A1) shows an elastic response, which is generally typical for cross-linked materials (even though the systems under study are thermoplastic), as confirmed by the presence of a horizontal plateau. The addition of graphene does not affect the viscoelastic properties of all tested TPUs: indeed, G′ remains constant within the range of frequencies explored and decreases with increasing the nanofiller content. As already observed, this behavior can be ascribed to a lubrication effect induced by graphene sheets [18]: the only difference concerns the lack of a threshold of graphene concentration, which promotes the lubrication effect, at least within the investigated graphene concentration range. Indeed, a very small amount of nanofiller (0.08 mg mL^{-1}) is already capable to strongly lower the G′ values of the composite.

The complex viscosity curves, plotted in Fig. 6b, indicate that the viscosity decreases with increasing the graphene content; furthermore, the slope of the regression lines, which were used for interpolating viscosity data and giving an indication of the non-Newtonian behavior of the materials, remains constant for all the compositions investigated (Table 1). As already discussed for G′, these results further confirm the lubrication effect exerted by graphene and the unchanged viscoelastic behavior of all the nanocomposites with respect to the unfilled counterpart.

Fig. 7a plots G′ and G″ vs. frequency for the IPDI-BD system and for some of its nanocomposites. Unlike the HDI-BD systems previously discussed, the viscoelastic behavior of the unfilled polymer (sample IPDI-BD, B1) is substantially thermoplastic-like and the moduli are frequency-dependent. The presence of graphene induces some changes in the viscoelastic behavior of the nanocomposites: indeed, the crossover point is within the considered frequencies range for TPUs containing small amounts of graphene (0.11 mg mL^{-1}), whereas the moduli tend to diverge by

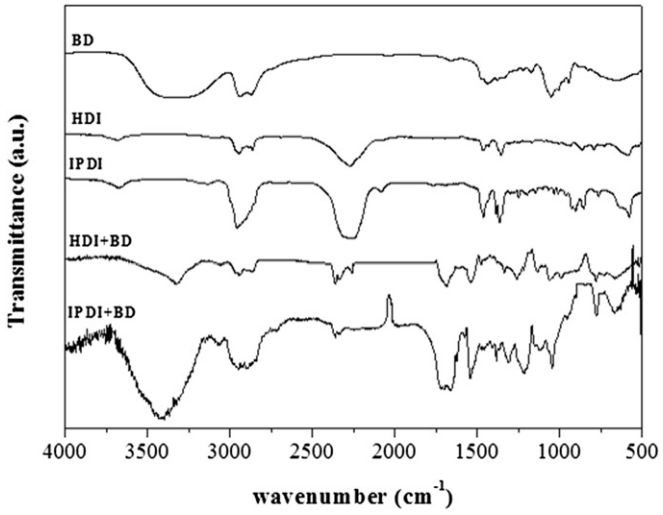

Fig. 4. FT-IR spectra of BD, HDI and IPDI monomers and of the corresponding polyurethanes (samples A1 and B1).

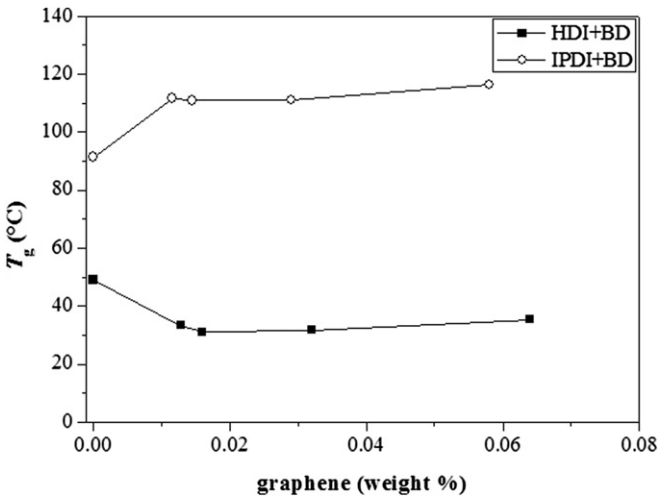

Fig. 5. T_g values (from DSC analysis) of HDI-BD and IPDI-BD polyurethane systems, as a function of graphene concentration.

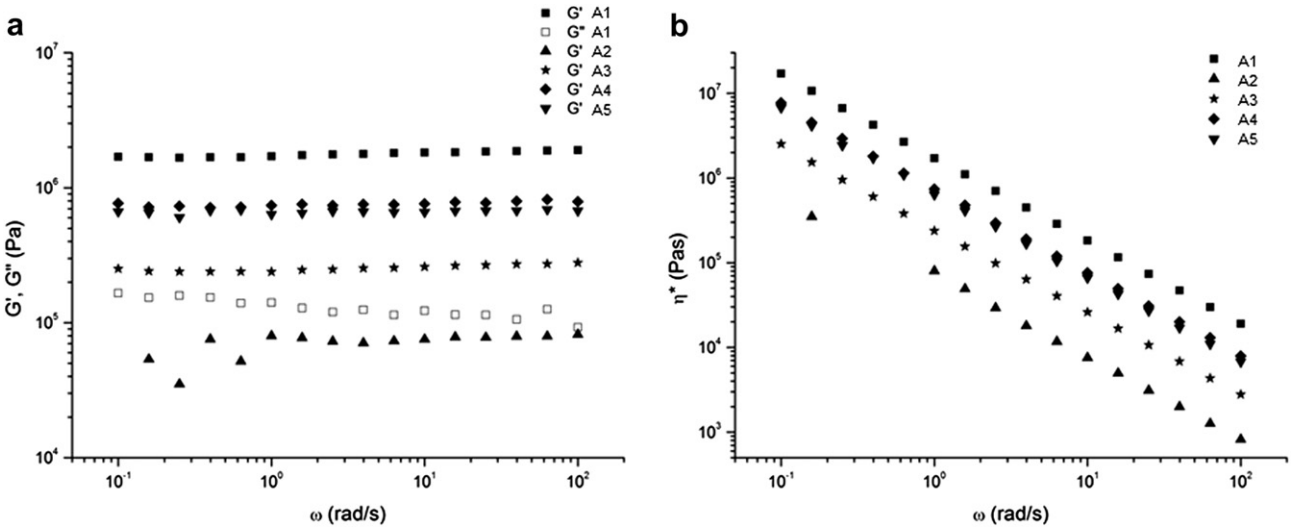

Fig. 6. Viscoelastic moduli (a) and complex viscosity (b) vs. frequency for some investigated TPU systems (their compositions are listed in Table 1).

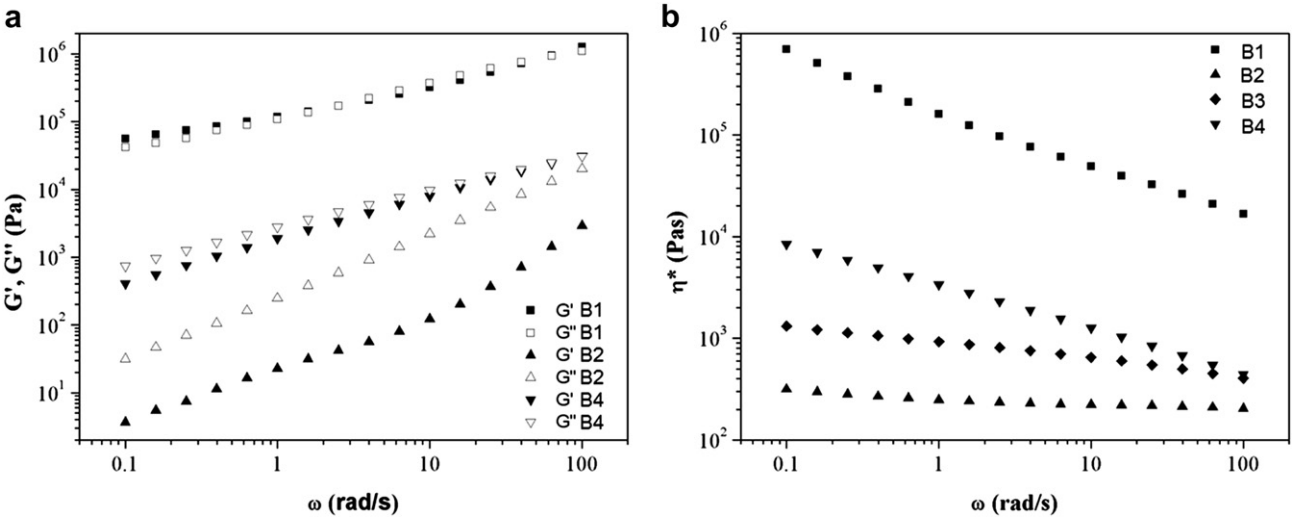

Fig. 7. Viscoelastic moduli (a) and complex viscosity (b) as a function of frequency for some investigated TPU systems (their compositions are listed in Table 1).

increasing the nanofiller content. Furthermore, it can be observed that both G′ and the complex viscosity (Fig. 7b) abruptly fall off in presence of graphene, thus confirming a lubrication effect of the nanofiller for all the concentrations investigated. The viscosity at 0.1 rad/s decreases by more than three orders of magnitude moving from the TPU matrix (10^6 Pa s) to the composite having the highest graphene content (1.14 mg mL^{-1}, 300 Pa s). A significant change in viscoelastic behavior is also evident, since the plastic IPDI-BD system becomes Newtonian at high graphene contents, i.e. η^* becomes independent of the frequency (the parameters of the regression lines are collected in Table 2).

4. Conclusions

Graphene and graphene nanoribbon/polyurethane thermoplastic nanocomposites were obtained through the polymerization of 1,4-butanediol with 1,6-hexane diisocyanate or isophorone diisocyanate. Very high nanofiller concentrations were achieved by directly sonicating graphite in the starting diols and diisocyanates, exploiting a strategy we have already proposed for preparing polymer nanocomposites [19]. In particular, it is worth mentioning that, at variance to the most commonly reported methods, which involve the oxidation of graphite to graphite oxide, its dispersion to get graphene oxide and the reduction of this latter, the process here reported does not make use of any chemical manipulation.

Furthermore, it should be highlighted that by the same method, a significant amount of graphene nanoribbons was also obtained in HDI, thus paving the way for their production through a much easier and effective technique than those reported in the literature so far.

The T_g values and the rheological features of the nanocomposites turned out to be strongly affected by the type of polyurethane system and by the concentration of the nanofiller used: indeed, graphene substantially acted as a lubricant for the HDI-BD system, whereas it was found to exert a reinforcing effect in the case of the IPDI-BD matrix.

Acknowledgments

S. Scognamillo thanks “RegioneAutonoma della Sardegna” for the financial support (“Master and Back” program). This work was partially financed by the Italian Ministry of University and Research (PRIN 2008).

References

[1] Lee C, Wei X, Kysar JW, Hone J. Science 2008;321:385–8.
[2] Balandin AA, Ghosh S, Bao W, Calizo I, Teweldebrhan D, Miao F. Lau CN.Nano Lett 2008;8(3):902–7.
[3] Bolotin KI, Sikes KJ, Jiang Z, Klima M, Fudenberg G, Hone J, et al. Solid State Comm 2008;146(9–10):351–5.
[4] Stoller MD, Park S, Zhu Y, An J, Ruoff RS. Nano Lett 2008;8(10):3498–502.
[5] Singh V, Joung D, Zhai L, Das, Khondaker SI, Seal S. Progr Mater Sci 2011;56(8):1178–271.
[6] Park S, Lee KS, Bozoklu G, Cai W, Nguyen ST, Ruoff RS. ACS Nano 2008;2(3):572–8.
[7] Stankovich S, Piner RD, Chen X, Wu N, Nguyen ST, Ruoff RS. J Mater Chem 2006;16(2):155–8.
[8] Stankovich S, Piner RD, Nguyen ST, Ruoff RS. Carbon 2006;44(15):3342–7.
[9] Coleman JN. J Acc Chem Res 2012. http://dx.doi.org/10 1021/ar 300009f.
[10] Hernandez Y, Nicolosi V, Lotya M, Blighe FM, Sun ZY, De S, et al. Nat Nanotechnol 2008;3(9):563–8.
[11] Liu N, Luo F, Wu H, Liu Y, Zhang C. Adv Funct Mater 2008;18(10):1518–25.
[12] Behabtu N, Lomeda JR, Green MJ, Higginbotham AL, Sinitskii A, Kosynkin DV, et al. Nat Nanotechnol 2010;5(6):406–11.
[13] Khan U, O'Neill A, Lotya M, De S, Coleman JN. Small 2010;6(7):864–71.
[14] Lotya M, Hernandez Y, King PJ, Smith RJ, Nicolosi V, Karlsson LS, et al. J Am Chem Soc 2009;131(10):3611–20.
[15] Blake P, Brimicombe PD, Nair RR, Booth TJ, Jiang D, Schedin F, et al. Nano Lett 2008;8(6):1704–8.
[16] Green AA, Hersam MC. Nano Lett 2009;9(12):4031–6.
[17] Nuvoli D, Valentini L, Alzari V, Scognamillo S, Bittolo Bon S, Piccinini M, et al. J Mater Chem 2011;21(10):3428–31.
[18] Alzari V, Nuvoli D, Scognamillo S, Piccinini M, Gioffredi E, Malucelli G, et al. J Mater Chem 2011;21(24):8727–33.
[19] Alzari V, Nuvoli D, Sanna R, Scognamillo S, Piccinini M, Kenny JM, et al. J Mater Chem 2011;21(41):16544–9.
[20] Albertsson AC, Ljungquist OJ. J MacromolSciChem 1986;23(3):411–22.
[21] Albertsson AC, Ljungquist OJ. Acta Polym 1988;39(1–2):95–104.
[22] Russo S, Mariani A, Ignatov VN, Ponomarev II. Macromolecules 1993;26(18):4984–5.
[23] Reed AM, Gilding DK. Polymer 1981;22(4):499–504.
[24] Stirna UK, Tupureina VV, Sevast'yanova IV, Dzene AV, Misane MM, Vilsone DM. Polym Sci Ser A 2003;45:765–72.
[25] Stirna UK, Tupureina VV, Misane MM, Dzene AV, Sevast'yanova IV. Polym Sci Ser A 2002;44:510–7.
[26] Koyama N, Doi J. Macromolecules 1996;29(18):5843–51.
[27] Monticelli O, Mendichi R, Bisbano S, Mariani A, Russo S. Macromol Chem Phys 2000;201(16):2123–7.
[28] Son YW, Cohen ML, Louie SG. Phys Rev Lett 2006;97(21):216803–6.
[29] Nakada K, Fujita M, Dresselhaus G, Dresselhaus MS. Phys Rev B 1996;54(24):17954–61.
[30] Son YW, Cohen ML, Louie SG. Nature 2006;444:347–9.
[31] Trauzettel B, Bulzev DV, Loss D, Burkarol G. Nat Phys 2007;3(3):192–6.
[32] Wang X, Ouyang Y, Jiao L, Wang H, Xie L, Wu J, et al. Nat Nanotechnol 2011;6(9):563–7.
[33] Li D, Müller MB, Gilje S, Kaner RB, Wallace GG. Nat Nanotechnol 2008;3(2):101–5.
[34] Lotya M, King PJ, Khan U, De S, Coleman JN. ACS Nano 2010;4(6):3155–62.
[35] Li X, Wang X, Zhang L, Lee S, Dai H. Science 2008;319:1229–32.
[36] Wu ZS, Ren W, Gao L, Liu B, Zhao J, Cheng HM. Nano Res 2010;3(1):16–22.
[37] Jiao L, Wang X, Diankov G, Wang H, Dai H. Nat Nanotechnol 2010;5(5):321–5.
[38] Terrones M, Botello-Mendez AR, Campos-Delgado J, Lopez-Urias F, Vega-Cantu YI, Rodriguez-Macias FJ, et al. Nano Today 2010;5(4):351–72.
[39] Valentini L, Trentini M, Mengoni F, Alongi J, Armentano I, Ricco L, et al. Diam Relat Mater 2007;16(3):658–63.